

## Search for Light Neutron-Rich Isotopes in Stopped Pion Absorption

Yu. B. Gurov, L. Yu. Korotkova, S. V. Lapushkin, R. V. Pritula,  
V. G. Sandukovsky, M. V. Tel'kushev, B. A. Chernyshev\*, and T. D. Schurenkova

*National Research Nuclear University MEPhI, Kashirskoe sh. 31, Moscow, 115409 Russia*

Received November 25, 2015

**Abstract**—The results based on the spectroscopy of superheavy hydrogen isotopes ( $^4\text{--}^7\text{H}$ ), heavy helium isotopes ( $^6,^7\text{He}$ ), and heavy lithium isotopes ( $^7\text{--}^{12}\text{Li}$ ) produced in stopped pion absorption by light nuclei were analyzed. Search for nuclear states was performed in inclusive and correlation measurements of missing mass spectra. A broad range of excitation energies studied in correlation measurements provided the possibility of search for isobaric analog states and cluster resonances. A comparison with experimental and theoretical results of other authors was conducted.

**DOI:** 10.1134/S1063778816040116

### 1. INTRODUCTION

Investigation of the structure of levels of light neutron-rich nuclei lying in the vicinity of the nucleon drip line is one of the main lines of the development of modern nuclear physics [1, 2]. A relatively small number of nucleons in them makes it possible to describe microscopically their properties and, as consequence, to test nuclear models and nucleon–nucleon potentials.

The majority of information about the spectroscopy of superheavy hydrogen isotopes and heavy helium and lithium isotopes was obtained in heavy-ion reactions, in particular, in those induced by radioactive beams (see [1–5] and references therein). However, data on excitation energies and widths of levels are contradictory for the majority of helium and lithium isotopes and are scanty for highly excited states. In this situation, it is natural to invoke new approaches to searches for exotic states.

A method for studying, by mean of reactions involving the absorption of stopped negatively charged pions, the structure of levels of light nuclei lying in the vicinity of the nucleon drip line was developed in a series of experiments at the synchrocyclotron of the Petersburg Nuclear Physics Institute (PNPI) [6–8]. The first ever observations of the superheavy hydrogen isotope  $^5\text{H}$  [7] and the ground state of  $^{10}\text{Li}$  [8] stand out among the physics results obtained in those investigations.

The absence of errors stemming from the energy resolution and from the angular spread of the beam is

a distinctive feature of this method. In the initial state, the momentum of the system being considered is zero. The uncertainty in the energy is due exclusively to the difference in the pionic-atom binding energy; for light nuclei, it does not exceed 100 keV.

A large energy deposition upon pion absorption leads to the production of several fast nuclear particles. In reactions involving the production of charged particles, the residual nucleus possesses a neutron excess. The production of such nuclei in two- and three-body reaction channels manifests itself as peaks in the spectra of missing masses with respect to detected particles. It is noteworthy that a sizable contribution to pion absorption by nuclei comes from quasifree processes, where the nucleons of the residual nucleus do not participate directly in the respective reaction. This favors the production of loosely bound and quasistationary states in three-body reaction channels. The possibility of studying, in a single experiment, a significant number of isotopes in detecting various particles and their pairs is an important advantage of the method being considered.

The results obtained at the PNPI accelerator underlay the program aimed at studying neutron-rich nuclei and implemented by means of reactions induced by the  $\pi^-$ -meson beam of the Los Alamos Meson Physics Facility (LAMPF). In the present article, we analyze spectroscopic data on superheavy hydrogen isotopes ( $^4\text{--}^7\text{H}$ ) [9, 10], heavy helium isotopes ( $^6,^7\text{He}$ ) [11–14], and heavy lithium isotopes ( $^7\text{--}^{12}\text{Li}$ ) [15–18] from an experiment already performed.

---

\*E-mail: [chernyshev@mephi.ru](mailto:chernyshev@mephi.ru)

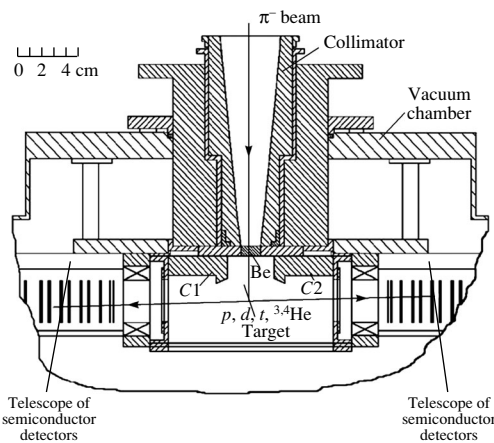


Fig. 1. Layout of the experimental setup used.

## 2. DESCRIPTION OF THE EXPERIMENT

The experiment described here was performed with the aid of a double-arm semiconductor spectrometer [19]. The layout of the experimental setup used is presented in Fig. 1. A beam of 30 MeV negatively charged pions traversed a beryllium moderator and underwent stopping in a thin target. The rate of pion stopping in targets was about  $6 \times 10^4 \text{ s}^{-1}$ . In the experiment, use was made of five targets:  $^9\text{Be}$ ,  $^{10,11}\text{B}$ , and  $^{12,14}\text{C}$ . They were manufactured in the form of disks 26 mm in diameter and about  $25 \text{ mg cm}^{-2}$  in thickness. Collimators C1 and C2 were employed to suppress the background of secondary particles originating from the moderator and chamber walls.

Charged secondaries, including the hydrogen isotopes  $p$ ,  $d$ , and  $t$  and the helium isotopes  $^3,^4\text{He}$  produced upon absorption in the targets, were detected by two multilayered semiconductor telescopes arranged at an angle of  $180^\circ$  with respect to each other. Either telescope consisted of two Si(Au) semiconductor detectors 100 and  $450 \mu\text{m}$  thick and fourteen Si(Li) semiconductor detectors about 3 mm thick. The working area of the sensitive region of all detectors was  $8 \text{ cm}^2$ . The Si(Au) semiconductor detectors did not have sizable insensitive regions. The thickness of the insensitive (lithium) layer in the Si(Li) semiconductor detectors was about  $100 \mu\text{m}$ .

The total thickness of the sensitive layer in either telescope was about 43 mm, which was in excess of the ranges of all charged nuclear particles produced in the absorption reaction on the targets used in the experiment. As a result, a high energy resolution ( $\Delta E$ ) was reached over the whole measured range of detected-particle energies. The FWHM  $\Delta E$  value was 0.5 MeV for singly charged particles ( $p$ ,  $d$ , and  $t$ ) and 2 MeV for doubly charged particles ( $^3,^4\text{He}$ ). The

error in the absolute matching of the energy scale did not exceed 0.1 MeV.

In correlation measurements, the missing-mass ( $MM$ ) resolution  $\Delta_{MM}$  is determined by three factors: the uncertainties in the measurement of energies for either particle and the uncertainty in the opening angle between the outgoing particles because of a finite angular acceptance of the telescopes. For pairs of detected singly charged particles,  $\Delta_{MM} \approx 1.0 \text{ MeV}$ , while, for pairs of hydrogen and helium isotopes, the respective value is  $\Delta_{MM} \sim 3.0 \text{ MeV}$ . For all pairs of singly charged particles, with the exception of  $pp$  pairs, the absolute matching of the  $MM$  scale is accurate to within 0.1 MeV. For the remaining particle pairs, the respective error does not exceed 0.2 MeV.

For a more detailed description of the spectrometer and experimental procedure used, the interested reader is referred to [9, 19].

## 3. RESULTS AND DISCUSSION

In order to separate the states under study, we used the least squares method in approximating the experimental missing mass ( $MM$ ) spectra by the sum of Breit–Wigner distributions and  $n$ -particle phase-space distributions ( $n \geq 3$  for inclusive measurements and  $n \geq 4$  for correlation measurements). In order to describe resonance levels in the energy range of  $E_r < 1 \text{ MeV}$ , we used threshold Breit–Wigner distributions [20].

### 3.1. Superheavy Hydrogen Isotopes $^4\text{--}^7\text{H}$

A detailed review of our results concerning the search of the superheavy hydrogen isotopes  $^4\text{--}^7\text{H}$  in stopped-pion absorption by  $^9\text{Be}$  and  $^{11}\text{B}$  nuclei was given in [9]. Among these results, the following deserve particular attention.

The missing-mass spectrum measured in the reaction  $^9\text{Be}(\pi^-, dt)^4\text{H}$  exhibits three states of  $^4\text{H}$  that have the following values of the resonance parameters  $E_r$  and  $\gamma$  (here,  $E_r$  is the resonance energy and  $\gamma^2$  is the reduced resonance width): 1.6(1) and 0.4(1) MeV, 3.4(1) and 0.4(1) MeV, and 6.0(1) and 0.5(1) MeV. In relation to the results obtained in ion-beam experiments (see [21, 22] and references therein), a greater number of levels is observed in the above reaction, the ground state of  $^4\text{H}$  being more strongly bound. Yet another piece of evidence of the existence of a narrow  $^4\text{H}$  level [at an energy of 3.5(3) MeV with a width less than 0.5 MeV] was found in the reaction  $^{10}\text{B}(\pi^-, t^3\text{He})X$  [10].

Either of the isotopes  $^5\text{H}$  and  $^6\text{H}$  was observed in two reaction channels: the former in  $^9\text{Be}(\pi^-, pt)^5\text{H}$

and  ${}^9\text{Be}(\pi^-, dd){}^5\text{H}$  and the latter in  ${}^9\text{Be}(\pi^-, pd){}^6\text{H}$  and  ${}^{11}\text{Be}(\pi^-, p^4\text{He}){}^6\text{H}$ . For these nuclei, the weighted-mean values of the resonance parameters are given in Table 1. The values of the resonance energies for the most strongly bound states of  ${}^5\text{H}$  and  ${}^6\text{H}$  are substantially higher in our measurements than in ion experiments. According to the measurements in radioactive beams, the resonance energy of the  ${}^5\text{H}$  ground state ranges from 1.7 MeV in [23] to 3 MeV in [24]. In two heavy ion experiments, a value of  $E_r \cong 2.7$  MeV was obtained for the ground state of  ${}^6\text{H}$  [25, 26]. As a possible explanation for this discrepancy, it can be hypothesized that the production of  $J^\pi = 1/2^+$  states is suppressed in stopped-pion absorption.

The observation of excited levels of the isotopes  ${}^{6,7}\text{H}$  was an important result of our measurements. The resonance energies of these states exceed the threshold for isotope decays to free nucleons. The excitations of these free-nucleon systems prove to be rather high, reaching a value of about 2 MeV per nucleon. The statement that such highly excited states do indeed exist was obtained in studying the reaction  ${}^7\text{Li}({}^3\text{He}, p^3\text{He})X$  at  $E_{3\text{He}} = 120$  MeV [27]. The measured missing-mass spectrum showed two relatively narrow ( $\Gamma \leq 2$  MeV) states of  ${}^6\text{He}$  at excitation energies of  $E_x \sim 32.0$  and  $35.7$  MeV.

For nuclei in the vicinity of the nucleon drip line, traditional magic numbers disappear, giving way to new ones [2]. In particular, it follows from experimental data on the spectroscopy of helium, lithium, and beryllium isotopes that  $N = 6$  becomes a neutron magic number instead of  $N = 8$ . Therefore, it is natural to expect that  ${}^7\text{H}$  has the highest binding energy among the superheavy hydrogen isotopes. However, only indications of the possible existence of this nucleus have been obtained thus far [2].

In an experiment performed at LAMPF, the search for the isotope  ${}^7\text{H}$  was performed in  $MM$  spectra for two channels:  ${}^9\text{Be}(\pi^-, pp)X$  and  ${}^{11}\text{B}(\pi^-, p^3\text{He})X$ . No statistically significant evidence of the existence of  ${}^7\text{H}$  states was obtained in those measurements. Nevertheless, it is worth noting that a structure in the vicinity of  $E_r \sim 0$  exists in the missing-mass spectrum of the reaction  ${}^{11}\text{B}(\pi^-, p^3\text{He})X$ . However, a quantitative analysis of this region is complicated by a small volume of the accumulated data sample and by an insufficient energy resolution in this channel.

### 3.2. Heavy Helium Isotopes ${}^{6,7}\text{He}$

Along with the superheavy hydrogen isotopes, the heavy helium isotopes feature a maximum relative excess of neutrons with respect to protons. The

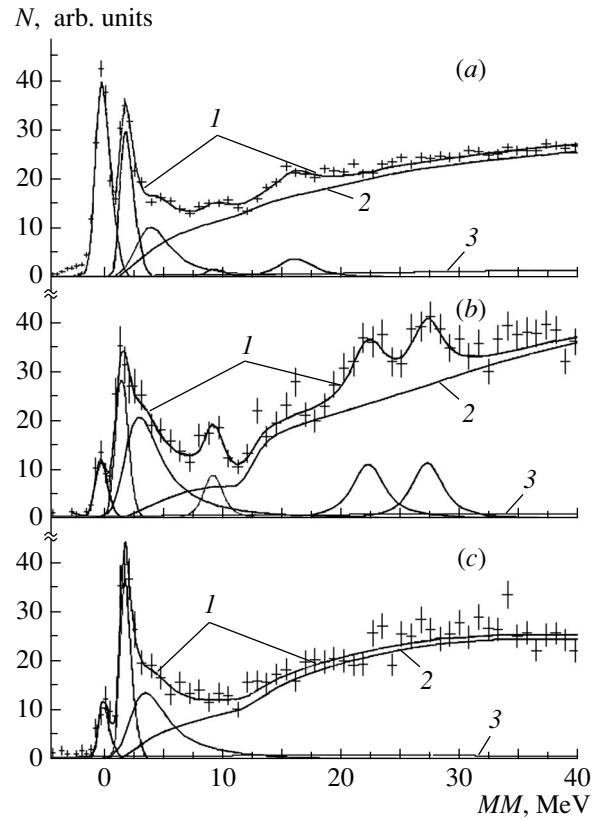


**Fig. 2.** Missing-mass ( $MM$ ) spectrum in the reactions (a)  ${}^{11}\text{B}(\pi^-, dt){}^6\text{He}$ , (b)  ${}^{10}\text{B}(\pi^-, pt){}^6\text{He}$ , and (c)  ${}^{10}\text{B}(\pi^-, dd){}^6\text{He}$ . The points with error bars stand for experimental data. Curves 1 represent a total description involving Breit–Wigner distributions and (2) the summed phase-space distribution. Curve 3 corresponds to the background of random coincidences.

${}^6\text{He}$  nucleus is the lightest nucleus that possesses a neutron halo. Investigation of the properties of the isotope  ${}^6\text{He}$  in the ground state and in excited states is of importance for obtaining deeper insight into the properties of other exotic light two- and three-particle nuclear systems. The properties of the  ${}^7\text{He}$  nucleus, which is unstable against nucleon emission, is of interest for studying the properties of nuclear resonances in a continuum.

**Table 1.** Parameters of the  ${}^5\text{H}$  and  ${}^6\text{H}$  states

$E_r$ , MeV	$\Gamma$ , MeV	$E_r$ , MeV	$\Gamma$ , MeV
${}^5\text{H}$		${}^6\text{H}$	
5.5(2)	5.4(5)	6.7(7)	5.5(2.0)
10.6(3)	6.8(5)	10.7(7)	4(2)
18.5(4)	4.8(1.3)	15.1(7)	3(2)
26.7(4)	3.6(1.3)	21.4(4)	3.5(1.0)

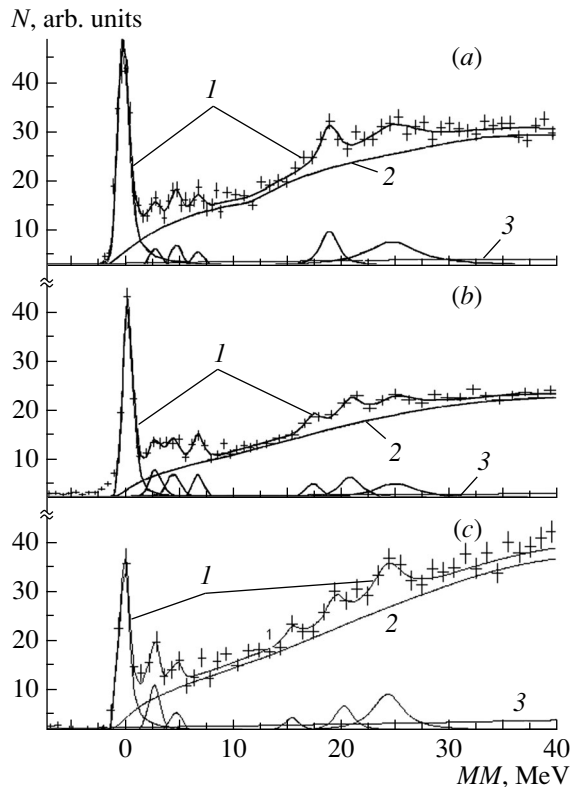


Fig. 3. As in Fig. 2, but for the reactions (a)  $^{11}\text{B}(\pi^-, pt)^7\text{He}$ , (b)  $^{11}\text{B}(\pi^-, dd)^7\text{He}$ , and (c)  $^{10}\text{B}(\pi^-, pd)^7\text{He}$ .

In our experiment, the structure of levels in the  $^6\text{He}$  nuclei was studied in detail in stopped pion absorption by  $^9\text{Be}$  and  $^{10,11}\text{B}$  nuclei.

Table 2. Parameters of excited states of the  $^6\text{He}$  nucleus

$E_x$ , MeV	$\Gamma$ , MeV	Reaction
1.80(3)	0.11(2)	1, 2, 3
3.5(2)*	3.1(4)*	1, 2, 3
9.3(2)*	1.0(4)*	1, 2
15.8(6)	1.1(6)	4
15.9(5)	3.2(7)	1
20.9(3)	3.2(6)	4
22.1(1.0)	2.7(1.4)	2
27.0(8)	2.5(1.1)	2
31.1(1.0)	6.9(2.3)	4

Figures 1, 2, 3, and 4 stand for the reactions  $^{11}\text{B}(\pi^-, dt)^6\text{He}$ ,  $^{10}\text{B}(\pi^-, pt)^6\text{He}$ ,  $^{10}\text{B}(\pi^-, dd)^6\text{He}$ , and  $^9\text{Be}(\pi^-, t)t + t$ , respectively.

\* Weighted-mean values.

In correlation measurements, the search for  $^6\text{He}$  states was performed in MM spectra measured in the reactions  $^{11}\text{B}(\pi^-, dt)^6\text{He}$ ,  $^{10}\text{B}(\pi^-, pt)^6\text{He}$ , and  $^{10}\text{B}(\pi^-, dd)^6\text{He}$  (see Fig. 2). In all of these spectra, the ground-state mass of  $^6\text{He}$  was taken to be a reference point. All of the spectra exhibit structures associated with three-body channels involving the production of  $^6\text{He}$  in the ground state and in excited states. For  $E^*$  values above the threshold for the decay  $^6\text{He}^* \rightarrow t + t$  (12.305 MeV), the search for resonance states in the system of two tritons was performed in the reaction  $^9\text{Be}(\pi^-, t)t + t$ . One of the two tritons from  $^6\text{He}$  decay was detected in those measurements. The values obtained in all measurements for the parameters of  $^6\text{He}$  excited states are presented in Table 2.

In the region of low excitation energies, yet another low-lying state of  $^6\text{He}$  manifests itself in all three reactions in addition to the ground and first excited states. The weighted-mean values of the parameters of this state are  $E_x = 3.5(3)$  MeV and  $\Gamma = 3.1(4)$  MeV. A resonance whose parameters have close values of  $E_x = 4(1)$  MeV and  $\Gamma = 4(1)$  MeV was observed in the reaction  $^6\text{Li}(^7\text{Li}, ^7\text{Be})^6\text{He}$  induced by a beam of 455 MeV  $^6\text{Li}$  ions [28]. The authors of [28] assumed that the state that they observed is a candidate for a soft dipole resonance.

A state of width  $\Gamma = 1.0(4)$  MeV at  $E_x = 9.3(2)$  MeV was first observed in the reactions  $^{10}\text{B}(\pi^-, pt)X$  and  $^{11}\text{B}(\pi^-, dt)X$ . A level at  $E_x = 9.7(2)$  MeV was observed in the reaction  $^6\text{Li}(d, ^2\text{He})^6\text{He}$ , but its width is substantially larger:  $\Gamma \sim 3$  MeV [29].

Above the threshold for  $^6\text{He}$  decay to two tritons, rather narrow levels are observed in three reaction channels. Two states at  $E_x \sim 15$  MeV have close excitation energies but differ markedly in width (see Table 2), and this may be indicative of different nature of their formation. This assumption is supported by the results reported in [30], where the state of width  $\Gamma = 4(2)$  MeV at  $E_x = 15.5(5)$  MeV is associated with the excitation of a giant dipole resonance. The excited  $^6\text{He}$  state characterized by an excitation energy of  $E_x = 27.0(8)$  MeV and a width of  $\Gamma = 2.5(1.1)$  MeV and identified by us in the channel  $^{10}\text{B}(\pi^-, pt)^6\text{He}$  was observed for the first time.

Search for  $^7\text{He}$  states was performed in correlation measurements of MM spectra in the reactions  $^{11}\text{B}(\pi^-, pt)^7\text{He}$ ,  $^{11}\text{B}(\pi^-, dd)^7\text{He}$ , and  $^{10}\text{B}(\pi^-, pd)^7\text{He}$  (see Fig. 3). The sum of the  $^6\text{He}$  and  $n$  masses was taken to be a reference point for all of these spectra. All spectra show structures associated with three-body channels involving the production of  $^7\text{He}$  in the

ground state and in excited states. The weighted-mean values obtained for the parameters of excited states of  ${}^7\text{He}$  are given in Table 3.

Our measurements did not reveal any indication of the existence of a  ${}^7\text{He}$  level that would be characterized by an anomalously low excitation energy (0.55 MeV) and which was found in [31]. An upper bound on the contribution of this state to the measured peak at  $E_x \sim 0$  MeV did not exceed 15% for all of the reactions studied in our experiment.

In the excitation-energy range of  $2.5 \leq E_x \leq 8$  MeV, the spectra in question show three narrow states of  ${}^7\text{He}$ . The existence of precisely three excited states in this range was predicted in several theoretical studies (see [32, 33] and references therein). In the order of increasing energy, the spin-parity assignments of the levels were  $J^\pi = 3/2^-$  (ground state),  $1/2^-$ ,  $5/2^-$ , and  $3/2^-$ . The theoretical predictions for their excitation energies and widths in those studies were markedly different. Our data lie most closely to the results reported in [33]:  $(E_x, \Gamma) = (3.27 \text{ MeV}, 2.7 \text{ MeV})$ ,  $(3.9 \text{ MeV}, 0.94 \text{ MeV})$  and  $(5.2 \text{ MeV}, 1.2 \text{ MeV})$ . In this excitation-energy region, three states were observed only in [34], but the widths of those states (about 2 MeV) were substantially larger.

In the region of high excitation energies above the threshold for the decay  ${}^7\text{He} \rightarrow t + t + n$  ( $E_x = 11.9$  MeV), our measurements revealed for the first time relatively narrow states of  ${}^7\text{He}$ . In other experiments, only broad states of  ${}^7\text{He}$  at  $E_x \sim 20$  MeV were observed in this energy region [3, 29, 35]. The nature of these states remains unclear. We can only indicate that the level at  $E_x = 19.8(3)$  MeV lies in the vicinity of the threshold for the decay  ${}^7\text{He} \rightarrow t + p + 3n$  (18.56 MeV), but this state is not an isobaric analog of the superheavy hydrogen isotope  ${}^7\text{H}$ , since, in the reaction  ${}^{11}\text{B}(\pi^-, dd){}^7\text{He}$ , the isospin of the final-state nucleus may assume only one value of  $T = 3/2$ .

### 3.3. Lithium Isotopes ${}^7\text{--}{}^{12}\text{Li}$

The  ${}^{11}\text{Li}$  nucleus is the point on the nucleon drip line for lithium isotopes. The neighboring isotopes  ${}^{10}\text{Li}$  and  ${}^{12}\text{Li}$  are unstable against nucleon emission. It is worth noting that a vigorous development of the nuclear-physics branch that studies the properties of exotic nuclear states in the vicinity of the nucleon drip line began precisely after the discovery of the fact that the radius of  ${}^{11}\text{Li}$  is anomalously large [36]. A model based on the assumption that the  ${}^{11}\text{Li}$  nucleus has a neutron halo formed by two valence nucleons was proposed in order to explain this phenomenon [37]. In order to analyze  ${}^{11}\text{Li}$  as a three-body system ( ${}^9\text{Li} +$

**Table 3.** Parameters of  ${}^7\text{He}$  excited states

$E_x$ , MeV	$\Gamma$ , MeV	Reaction
3.1(1)*	$\leq 0.5$	1, 2, 3
4.9(2)*	$\leq 0.5$	1, 2, 3
6.7(2)*	$\leq 0.5$	1, 2
16.9(5)*	1.0(3)*	2, 3
19.8(3)*	1.5(3)*	1, 2, 3
24.8(4)*	4.6(7)*	1, 2, 3

Figures 1, 2, and 3, stand for the reactions  ${}^{11}\text{B}(\pi^-, pt){}^7\text{He}$ ,  ${}^{11}\text{B}(\pi^-, dd){}^7\text{He}$ , and  ${}^{10}\text{B}(\pi^-, pd){}^7\text{He}$ , respectively.

\* Weighted-mean values.

$n + n$ ), one needs information about the properties of the  $(n + n)$  and  $({}^9\text{Li} + n)$  two-body subsystems. The properties of the latter are directly related to the properties of the isotope  ${}^{10}\text{Li}$ . The properties of heavier lithium isotopes (in particular,  ${}^{12}\text{Li}$ ), which lie beyond the nucleon drip line, are also of interest for the development of models that intended for describing the properties of these exotic nuclear systems.

In our experiment, the structure of levels of heavy lithium isotopes was studied in the following reaction channels:  ${}^{11}\text{B}(\pi^-, p){}^{10}\text{Li}$ ,  ${}^{12}\text{C}(\pi^-, pp){}^{10}\text{Li}$ ,  ${}^{14}\text{C}(\pi^-, pt){}^{10}\text{Li}$ ,  ${}^{14}\text{C}(\pi^-, dd){}^{10}\text{Li}$ ,  ${}^{14}\text{C}(\pi^-, pd){}^{11}\text{Li}$ , and  ${}^{14}\text{C}(\pi^-, pp){}^{12}\text{Li}$  [15, 17]. Figure 4 shows the results obtained for the reaction channels that provided the best statistical significance.

The ground state of  ${}^{10}\text{Li}$  is an  $s$ -wave virtual resonance for which the scattering length satisfies the condition  $a_s < -20$  fm [38, 39]. Within the resonance-energy formalism, this yields the constraint  $E_r < 0.05$  MeV. Information about the first excited state, which is a  $p$ -resonance, is less certain. The  $E_r$  values measured in different experiments lie in the range of  $0.3 \leq E_r \leq 0.7$  MeV [4, 15, 38–40]. Data on higher lying excited states of  ${}^{10}\text{Li}$  are scanty [4]. For  $E_r > 1.5$  MeV, they were obtained only in two studies. Six narrow states ( $\Gamma < 0.3$  MeV) in the range of  $1.4 \leq E_r \leq 5.7$  MeV were found in heavy-ion-transfer reactions [41]. A level at  $E_r \approx 0.7$  MeV was observed in the neutron-knockout reaction  $p({}^{11}\text{Li}, pn){}^{10}\text{Li}$  [42].

In our measurements, the ground state of  ${}^{10}\text{Li}$  was observed only in the reaction  ${}^{11}\text{B}(\pi^-, p){}^{10}\text{Li}$  (see Fig. 4a). The peak observed near  $MM \sim 0$  is described by a superposition of  $s$ - and  $p$ -wave states. Upon employing the Breit–Wigner formalism, we obtained the following values for the parameters of the states in question:  $E_r = 0.1(1)$  MeV and  $\Gamma < 0.1$  MeV for the ground state and  $E_r = 0.6(1)$  MeV

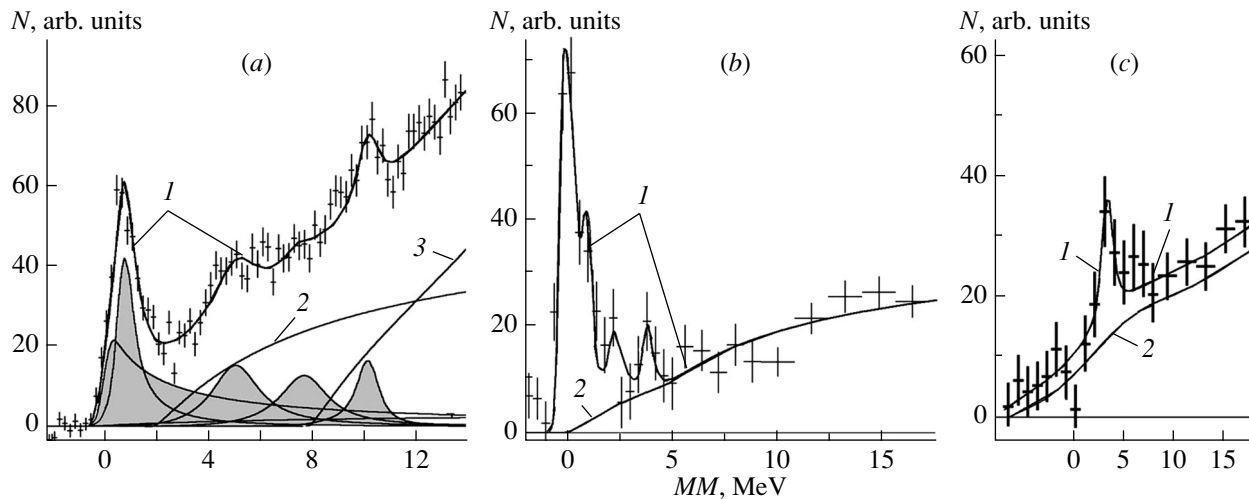


**Fig. 4.** Missing-mass ( $MM$ ) spectra measured in reactions leading to the production of the isotopes  $^{10-12}\text{Li}$ : (a)  $^{11}\text{B}(\pi^-, p)X$ , (b)  $^{14}\text{C}(\pi^-, pd)X$ , and (c)  $^{14}\text{C}(\pi^-, pp)X$ . The curves correspond to Breit–Wigner distributions. In Fig. 4a, curve 1 represents a complete description, while curves 2 and 3 stand for the phase-space distributions for  $^{11}\text{B}(\pi^-, p)^9\text{Li} + p + n$  and  $^{11}\text{B}(\pi^-, p)^7\text{He} + p + t$ , respectively. In Fig. 4b, curves 1 and 2 represent, respectively, a complete description and the summed phase-space distribution. In Fig. 4c, the notation for the curves is identical to that in Fig. 4b. The points with error bars stand for experimental data.

and  $\Gamma \sim 1$  MeV for the first excited state. These values agree with the results obtained in ion reactions [4, 38–40, 43]. In correlation measurements, we did not find any manifestations of the ground state. This may be due to a poorer resolution in  $MM$  and an insufficient statistical significance of the data in these reaction channels.

In all of the reactions under study, we observed excited states of  $^{10}\text{Li}$ . Their parameters are given in Table 4. The values obtained for the resonance parameters of the first excited state are compatible with the world-averaged data. Our measurements do not confirm the existence of the resonance at  $E_r = 1.4$  MeV, in contrast to [4, 41, 43, 44], where the

authors reported on the observation of indications of its existence. In the region of intermediate energies ( $2 < E_r < 7$  MeV), our measurements revealed three levels whose positions are close to those in [41], but the widths of these states are substantially larger in our measurements. For example, the level of highest excitation energy [ $E_r = 5.7(1)$  MeV and  $\Gamma = 0.2(1)$  MeV] in [41] is nearly one order of magnitude narrower than the level of width  $\Gamma \sim 1$  MeV observed at  $E_r = 6.1(1)$  MeV in reactions on  $^{14}\text{C}$  targets. This discrepancy may be indicative of different nature of these states.

In the region of high excitation energies lying above the threshold for the decay  $^{10}\text{Li} \rightarrow ^6\text{He} + t + n$  ( $E_r = 7.6$  MeV), our measurements revealed for the first time two levels that may be resonances in the  $^7\text{He} + t$  and  $^6\text{He} + ^4\text{H}$  systems.

The energy of separation of two neutrons from the isotope  $^{11}\text{Li}$ ,  $S_{2n} = 0.3693(6)$  MeV [45], is rather low, so that all excited states of  $^{11}\text{Li}$  are unstable against nucleon emission. Experimental results on their parameters are contained in the compilation presented in [5]. A level in the excitation-energy region around  $E_x \approx 1$  MeV was discovered in a large number of studies. However, the measured values of the excitation energy differ substantially, ranging from 0.6 [46] to 1.3 MeV [47]. The widths of these states are also different, 0.26 to 0.75 MeV. Higher lying levels were observed in a number of studies, but the spread of their parameters is substantially greater than the quoted measurement errors [5].

**Table 4.** Parameters of  $^{10}\text{Li}$  resonance states

$E_r$ , MeV	$\Gamma$ , MeV	Reaction
0.7(1)*	$\sim 0.5^*$	1, 2, 3, 4
2.2(1)	$\sim 1$	3
4.8(1)*	$\sim 1^*$	1, 2
6.1(1)*	$\sim 1^*$	3, 4
7.8(2)*	$\sim 2^*$	1, 2
10.1(1)	$\sim 0.5$	1

Figures 1, 2, 3, and 4 stand for the reactions  $^{11}\text{B}(\pi^-, p)^{10}\text{Li}$ ,  $^{12}\text{C}(\pi^-, pp)^{10}\text{Li}$ ,  $^{14}\text{C}(\pi^-, pt)^{10}\text{Li}$ , and  $^{14}\text{C}(\pi^-, dd)^{10}\text{Li}$ , respectively.

\* Weighted-mean values.

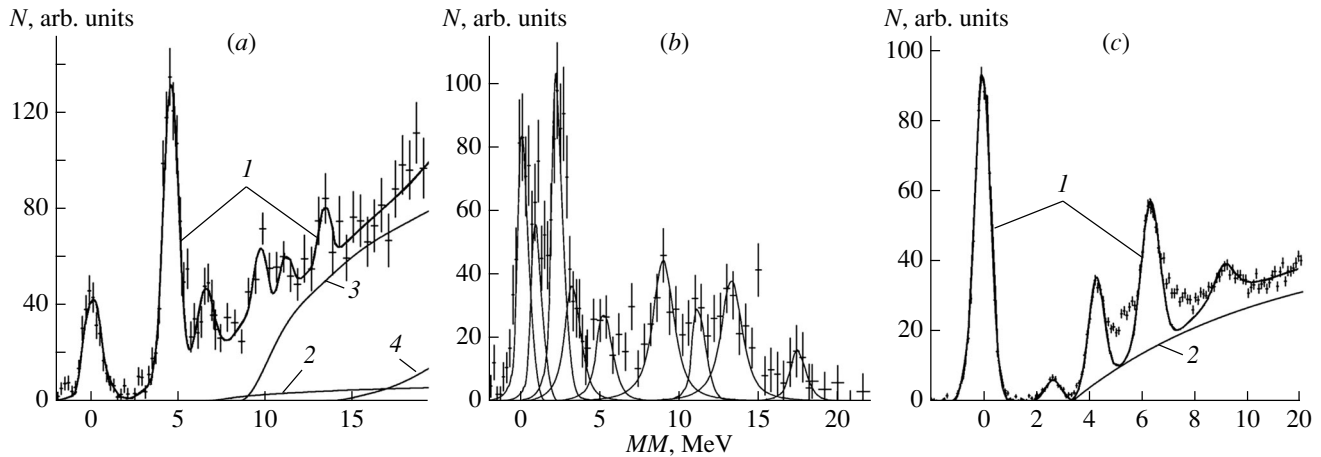


**Fig. 5.** Missing-mass ( $MM$ ) spectra measured in reactions leading to the production of the isotopes  ${}^{7-9}\text{Li}$ : (a)  ${}^{10}\text{B}(\pi^-, t)X$ , (b)  ${}^{12}\text{C}(\pi^-, dd)X$ , and (c)  ${}^{11}\text{B}(\pi^-, d)X$ . In Fig. 5a, curve 1 corresponds to a complete description, while curves 2, 3, and 4 represent the phase-space distributions for  ${}^{10}\text{B}(\pi^-, t){}^6\text{Li} + n$ ,  ${}^{10}\text{B}(\pi^-, t){}^5\text{He} + d$ , and  ${}^{10}\text{B}(\pi^-, t){}^5\text{Li} + 2n$ , respectively. In Figs. 5b and 5c, the notation for the curves is identical to that in Fig. 4b. The points with error bars stand for experimental data.

In our measurements, the search of  ${}^{11}\text{Li}$  production was performed in the missing-mass spectrum determined for the reaction  ${}^{14}\text{C}(\pi^-, pd){}^{11}\text{Li}$  (see Fig. 4b). A statistically satisfactory description of the spectrum is attained upon including three excited states of  ${}^{11}\text{Li}$  and setting their resonance parameters  $E_x$  and  $\Gamma$  to the following values: 0.92(15) MeV and about 0.3 MeV, 2.29(25) MeV and about 0.7 MeV, and 3.90(25) MeV and less than 0.2 MeV. The parameters of the first excited state are close to the results obtained in [43]. Within the experimental errors, the excitation energy of the second resonance state agrees with the results obtained in heavy ion  $\{2.47(7) \text{ MeV [48]}\}$  and fragmentation  $\{2.45(27) \text{ MeV [43]}\}$  reactions. However, the widths of the states in those experiments are substantially larger: 1.2(2) and 2.91(72) MeV, respectively. A narrow state at  $E_x = 3.90(25) \text{ MeV}$  was observed for the first time in our measurements.

For the first time, the ground state of  ${}^{12}\text{Li}$  was observed in the fragmentation of a radioactive  ${}^{14}\text{Be}$  beam of energy 304 MeV per nucleon [39]. This state is an  $s$ -wave virtual state for which the scattering length is  $a_s = -13.7(1.6) \text{ fm}$ . Later on, it was observed in the fragmentation of  ${}^{14}\text{Be}$  at the energy of 53.4 MeV per nucleon [49]. Two excited states of  ${}^{12}\text{Li}$  at resonance energies of 250(20) and 555(20) keV were also observed in that study. We note that the range of resonance energies measured in [49] was not wider than 4 MeV. Thus, experimental information about the structure of levels in  ${}^{12}\text{Li}$  is scanty.

In our measurements,  ${}^{12}\text{Li}$  production was studied by employing the missing mass spectrum in the reac-

tion  ${}^{14}\text{C}(\pi^-, pp){}^{12}\text{Li}$  (see Fig. 4c). This  $MM$  spectrum clearly shows a peak caused by a  ${}^{12}\text{Li}$  resonance state of width  $\Gamma = 1.1(4) \text{ MeV}$  at  $E_r = 4.0(2) \text{ MeV}$ . In the spectrum, there is no indication of the levels found in [39, 49] at low resonance energies.

Information about ground and low-lying excited states of lithium isotopes lighter than  ${}^{7-9}\text{Li}$  is quite comprehensive and is consistent [3, 4]. At the same time, data on high-lying excited states of these nuclei are incomplete, especially for  ${}^9\text{Li}$ . We note that observation of narrow highly excited states may provide information about the structure of nuclei in the vicinity of the nucleon drip line. For example, the level of  ${}^7\text{Li}$  at  $E_x = 11.24(30) \text{ MeV}$  [3] and the level of  ${}^8\text{Li}$  at  $E_x = 10.8222(55) \text{ MeV}$  [4] are isobaric analogs of the ground states of the helium isotopes  ${}^{7,8}\text{He}$ . Search for cluster resonances is yet another problem of interest. As follows from Ikeda's rule [50], such resonances may appear near the thresholds corresponding to the opening of decay channels. Many such resonances were observed in  $Z \geq 4$  nuclei [51]. For lithium isotopes, there is virtually no such information about the cluster structure of highly excited states.

In our experiment, the search for highly excited states of the isotopes  ${}^{7-9}\text{Li}$  was performed in inclusive and correlation measurements of pion absorption on  ${}^{10,11}\text{B}$  and  ${}^{12,14}\text{C}$  targets [16]. The results obtained in the reaction channels providing the highest statistical significance are given in Fig. 5. It should be noted that the spectrum in Fig. 5c was obtained after the subtraction of the summed phase-space distribution.

In all of the spectra studied here, manifestations high-lying states were found for lithium isotopes; some of them were observed for the first time.

States lying above the threshold for the decay  ${}^7\text{Li}^* \rightarrow {}^6\text{He} + n$  (9.9754 MeV) were observed in the reactions  ${}^{10}\text{B}(\pi^-, t)X$  (Fig. 5a) and  ${}^{12}\text{C}(\pi^-, dt)X$ . The isobaric analog state of  ${}^7\text{He}$  at  $E_x = 11.2(1)$  MeV with a width of  $\Gamma = 0.3(1)$  MeV was observed in the reaction  ${}^{10}\text{B}(\pi^-, t)X$ . A level of width  $\Gamma = 0.6(2)$  MeV at  $E_x = 13.4(2)$  MeV was also observed in this reaction. A state that has close resonance-parameter values of  $E_x = 13.7$  MeV and  $\Gamma \approx 0.5$  MeV was observed in the photonuclear reaction  ${}^7\text{Li}(\gamma, n){}^6\text{Li}$  [52]. A level of width  $\Gamma = 1.8(4)$  MeV at  $E_x = 10.3(1)$  MeV was discovered in the reaction  ${}^{12}\text{C}(\pi^-, dt)X$ . An indication of the existence of this level at  $E_x = 10.25$  MeV was obtained in another reaction of stopped-pion absorption,  ${}^9\text{Be}(\pi^-, nn)X$  [53].

Three highly excited levels of  ${}^8\text{Li}$  that lie higher than the isobaric analog state of  ${}^8\text{He}$  at  $E_x = 10.8222$  MeV were observed for the first time in the reaction  ${}^{12}\text{C}(\pi^-, dd)X$  (see Fig. 5b). Their parameters  $E_x$  and  $\Gamma$  have the following values: 11.2(2) and 0.4(2) MeV, 13.5(1) and 1.5(1) MeV, and 17.5(3) and 0.8(3) MeV. It should be noted that the production of these states in the reaction  ${}^{12}\text{C}(\pi^-, dd)X$  is forbidden by isotopic invariance. Their nature remains unknown. We note that the first two of these states lie near the thresholds for  ${}^8\text{Li}^*$  decays to  ${}^4\text{He} + d + n + n$  (10.8 MeV) and  ${}^4\text{He} + p + n + n + n$  (13.0 MeV). This proximity may suggest that the states being studied are multiparticle resonances.

Above the threshold for the decay  ${}^9\text{Li}^* \rightarrow {}^6\text{He} + t$  (7.59 MeV), a  ${}^9\text{Li}$  level of width  $\Gamma = 0.8(1)$  MeV at  $E_x = 9.1(2)$  MeV was observed for the first time in the reaction  ${}^{11}\text{B}(\pi^-, d)X$  (see Fig. 5c). Correlation measurements of the reaction  ${}^{14}\text{C}(\pi^-, dt)X$  provided an indication that there exists a  ${}^9\text{Li}$  level of width  $\Gamma \sim 0.6$  MeV at  $E_x \sim 10.5$  MeV. The cluster structure of  ${}^9\text{Li}$  was studied on the basis of a model in which use is made of the generalized-coordinate method [54]. In the range of  $1 < E_r < 4$  MeV, the model predicts the existence of four resonance states of  ${}^9\text{Li}$  in the  ${}^6\text{He} + t$  system, their spin-parities being  $J^\pi = 1/2^-$ ,  $3/2^-$ ,  $5/2^-$ , and  $7/2^-$ . This region corresponds to  ${}^9\text{Li}$  excitation energies in the range of  $8.6 < E_x < 11.6$  MeV. Therefore, we assume that the state at  $E_x = 9.1(2)$  MeV has a spin-parity of  $J^\pi = 1/2^-$  or  $3/2^-$  and that the state at  $E_x = 10.5$  MeV has a spin-parity of  $J^\pi = 5/2^-$  or  $7/2^-$ .

#### 4. CONCLUSIONS

We have examined results concerning the spectroscopy of superheavy hydrogen isotopes ( ${}^4\text{--}{}^7\text{H}$ ),

heavy helium isotopes ( ${}^6,{}^7\text{He}$ ), and heavy lithium isotopes ( ${}^7\text{--}{}^{12}\text{Li}$ ). These results have demonstrated that the use of stopped-pion absorption by nuclei in studying states of nucleon-rich nuclei that lie in the vicinity of the nucleon drip line is quite promising. The discovery of the ground states of the isotopes  ${}^5\text{H}$  and  ${}^{10}\text{Li}$  and the observation of highly excited states of the isotopes  ${}^5,{}^6\text{H}$ ,  ${}^6,{}^7\text{He}$ , and  ${}^{12}\text{Li}$  stand out among the results obtained by this method. The method in question can be used in future searches for and spectroscopic investigations of other exotic nuclear states such as multineutrons and the heavy helium isotopes  ${}^8,{}^9\text{He}$ .

#### ACKNOWLEDGMENTS

This work was supported in part by the Ministry of Education and Science of Russian Federation (grant no. 1729) and the Russian Science Foundation (grant no. 14-12-00079).

#### REFERENCES

1. B. Jonson, Phys. Rep. **389**, 1 (2004).
2. I. Tanihata, H. Savajols, and R. Kanungo, Prog. Part. Nucl. Phys. **68**, 215 (2013).
3. D. R. Tilley et al., Nucl. Phys. A **708**, 3 (2002).
4. D. R. Tilley et al., Nucl. Phys. A **745**, 155 (2004).
5. J. H. Kelley et al., Nucl. Phys. A **880**, 88 (2012).
6. M. G. Gornov et al., Nucl. Instrum. Methods Phys. Res. **225**, 42 (1984).
7. M. G. Gornov et al., Nucl. Phys. A **531**, 613 (1991).
8. A. I. Amelin et al., Sov. J. Nucl. Phys. **52**, 782 (1990).
9. Yu. B. Gurov, S. V. Lapushkin, B. A. Chernyshev, and V. G. Sandukovsky, Phys. Part. Nucl. **40**, 558 (2009).
10. Yu. B. Gurov, V. S. Karpukhin, S. V. Lapushkin, I. V. Laukhin, V. A. Pechkurov, V. G. Sandukovsky, and B. A. Chernyshev, Bull. Russ. Acad. Sci.: Phys. **73**, 139 (2009).
11. Yu. B. Gurov, V. S. Karpukhin, S. V. Lapushkin, I. V. Laukhin, V. A. Pechkurov, N. O. Poroshin, V. G. Sandukovsky, M. V. Tel'kushev, and B. A. Chernyshev, JETP Lett. **84**, 1 (2006).
12. Yu. B. Gurov, L. Yu. Korotkova, S. V. Lapushkin, R. V. Pritula, M. V. Tel'kushev, and B. A. Chernyshev, Bull. Russ. Acad. Sci.: Phys. **78**, 1108 (2014).
13. Yu. B. Gurov, V. S. Karpukhin, L. Yu. Korotkova, S. V. Lapushkin, T. I. Leonova, R. V. Pritula, B. A. Chernyshev, and T. D. Shchurenkova, Bull. Russ. Acad. Sci.: Phys. **79**, 478 (2015).
14. Yu. B. Gurov, L. Yu. Korotkova, S. V. Lapushkin, R. V. Pritula, V. G. Sandukovsky, M. V. Tel'kushev, and B. A. Chernyshev, JETP Lett. **101**, 69 (2015).
15. B. A. Chernyshev et al., Eur. Phys. J. A **49**, 68 (2013).
16. B. A. Chernyshev et al., Eur. Phys. J. A **50**, 150 (2014).
17. B. A. Chernyshev et al., Int. J. Mod. Phys. E **24**, 1550004 (2015).



18. Yu. B. Gurov, V. S. Karpukhin, L. Yu. Korotkova, S. V. Lapushkin, R. V. Pritula, V. G. Sandukovsky, and B. A. Chernyshev, *Bull. Russ. Acad. Sci.: Phys.* **79**, 474 (2015).
19. M. G. Gornov et al., *Nucl. Instrum. Methods Phys. Res. A* **446**, 461 (2000).
20. A. M. Lane and R. G. Thomas, *Rev. Mod. Phys.* **30**, 257 (1958).
21. D. V. Aleksandrov et al., *JETP Lett.* **62**, 18 (1995).
22. S. I. Sidorchuk et al., *Phys. Lett. B* **594**, 54 (2004).
23. A. A. Korshennikov et al., *Phys. Rev. Lett.* **87**, 092501 (2001).
24. M. Meister et al., *Nucl. Phys. A* **723**, 13 (2003).
25. D. V. Aleksandrov et al., *Sov. J. Nucl. Phys.* **39**, 323 (1984).
26. A. V. Belozorov et al., *Nucl. Phys. A* **460**, 352 (1986).
27. R. Franke et al., *Nucl. Phys. A* **433**, 351 (1985).
28. S. Nakayama et al., *Phys. Rev. Lett.* **85**, 262 (2000).
29. D. Frekers, *Nucl. Phys. A* **731**, 76 (2004).
30. F. P. Brady et al., *J. Phys. G* **10**, 363 (1984).
31. M. Meister et al., *Phys. Rev. Lett.* **88**, 102501 (2002).
32. S. C. Pieper, R. B. Wiringa, and J. Carlson, *Phys. Rev. C* **70**, 054325 (2004).
33. A. Volya and V. Zelevinsky, *Phys. Rev. Lett.* **94**, 052501 (2005).
34. A. H. Wuosmaa et al., *Phys. Rev. C* **72**, 061301(R) (2005).
35. T. Yamagata et al., *Phys. Rev. C* **69**, 044313 (2004).
36. I. Tanihata et al., *Phys. Rev. Lett.* **55**, 2676 (1985).
37. P. G. Hansen and B. Jonson, *Europhys. Lett.* **4**, 409 (1987).
38. H. B. Jeppesen et al., *Phys. Lett. B* **642**, 449 (2006).
39. Yu. Aksyutina et al., *Phys. Lett. B* **666**, 430 (2008).
40. P. Santi et al., *Phys. Rev. C* **67**, 024606 (2003).
41. H. G. Bohlen et al., *Prog. Part. Nucl. Phys.* **42**, 17 (1999).
42. T. Kobayashi et al., *Nucl. Phys. A* **616**, 223c (1997).
43. H. Simon et al., *Nucl. Phys. A* **791**, 267 (2007).
44. J. K. Smith et al., *Nucl. Phys. A* **940**, 235 (2015).
45. M. Wang et al., *Chin. Phys. C* **36**, 1603 (2012).
46. T. Nakamura et al., *Phys. Rev. Lett.* **96**, 252502 (2006).
47. A. A. Korshennikov et al., *Phys. Rev. C* **53**, R537 (1996).
48. H. G. Bohlen et al., *Z. Phys. A* **351**, 7 (1995).
49. C. C. Hall et al., *Phys. Rev. C* **81**, 021302 (2010).
50. K. Ikeda, N. Tagikawa, and H. Horiuchi, *Prog. Theor. Phys. Suppl.* **E68**, 464 (1968).
51. W. von Oertzen, M. Freer and Y. Kanada-En'yo, *Phys. Rep.* **432**, 42 (2006).
52. S. A. Siddiqui et al., *Nucl. Phys. A* **458**, 387 (1986).
53. B. Bassalleck et al., *Phys. Rev. C* **16**, 1526 (1977).
54. Y. Kanada-En'yo and T. Suhara, *Phys. Rev. C* **85**, 024303 (2012).